Electrostatic modes in collisional complex plasmas under microgravity conditions

V. V. Yaroshenko,* B. M. Annaratone, S. A. Khrapak, H. M. Thomas, and G. E. Morfill
Centre for Interdisciplinary Plasma Science, Max-Planck-Institut für Extraterrestrische Physik, D-85741 Garching, Germany

V. E. Fortov, A. M. Lipaev, V. I. Molotkov, and O. F. Petrov
Institute for High Energy Densities, Russian Academy of Sciences, 125412 Moscow, Russia

A. I. Ivanov and M. V. Turin
RSC "Energia," Korolev 141070, Russia
(Received 23 December 2003; published 2 June 2004)

A linear dispersion relation in a highly collisional complex plasma, including ion drift, was derived in the light of recent PKE-Nefedov wave experiment performed under microgravity conditions onboard the International Space Station. Two modifications of dust density waves with wave frequencies larger than the dust-neutral collision frequency were obtained. The relevance to the space observations was analyzed and a comparison of theory and observations was made for two different complex plasma domains formed by small and large microparticles. Good qualitative agreement is found between the measurements and the theoretical dispersion relations. This allows a determination of the basic complex plasma parameters.

DOI: 10.1103/PhysRevE.69.066401 PACS number(s): 52.27.Lw, 52.35.−g

I. INTRODUCTION

Complex plasmas are characterized by the presence of charged microparticles, besides the usual electron and ion species. Such particles usually accumulate charges that exceed the electron and ion charges by orders of magnitude, and in comparison have also much higher mass-to-charge ratios. Hence, the appearance of very low frequencies, characteristic for the charged microparticles, which move in space and time scales that differ vastly from the normal electron and ion scales, should be expected. Among the many new modes, the prime example is the electrostatic dust-acoustic wave, which is associated with dust number density perturbations, and the dust-lattice wave, which occurs as a result of coherent vibrations of microparticles organized in crystal-like structures. These modes have been extensively studied in recent years both theoretically and experimentally [1–14]. Recently, the first experiment on dust-acoustic waves performed under microgravity conditions onboard the International Space Station (ISS) and its theoretical interpretation were reported [15].

Laboratory complex plasmas are usually weakly ionized and thus are strongly collisional. Moreover, real complex plasmas are subjected to discharge electric fields, and as a result the ions acquire drifts due to these fields and stream through the more inertial microparticle component, leading to various kinds of streaming instabilities [16–19]. Incorporating all these effects simultaneously, we rederived the dispersion relation for the dust density perturbations, allowing us to consider a highly collisional regime, dust charge fluctuations, and ion drift [20]. Contrary to this previous work, where the dust modes of frequencies smaller than the characteristic frequency of the dust-neutral collisions were mostly discussed, the focus of the present paper is on the modifications of the dispersion relation when dust density perturbations have significantly higher frequencies and thus propagate at the phase velocities higher than the usual dust-acoustic velocity, in the range of small wave numbers. As follows from this paper, the results are directly applicable to some of the recent experiments performed under microgravity conditions onboard the International Space Station [21], namely, on dust density waves observed in a specific wave channel arising in a complex plasma under microgravity conditions.

II. THEORY

A. Basic equations

In this study of complex plasma waves, we consider a four-component collisional complex plasma, consisting of warm plasma electrons (subscript e), ions (subscript i), neutrals (subscript n), and cold charged monodisperse microparticles (subscript d). The plasma species obey the standard fluid equations

$$\frac{\partial v_e}{\partial t} + v_e \frac{\partial v_e}{\partial x} + \nu_{en} v_e + \frac{v_{Te}^2}{n_e} \frac{\partial n_e}{\partial x} = -\frac{e}{m_e} E, \tag{1}$$

$$\frac{\partial v_i}{\partial t} + v_i \frac{\partial v_i}{\partial x} + \frac{v_{Ti}^2}{n_i} \frac{\partial n_i}{\partial x} + \nu_{in} v_i + \nu_{id}(v_i - v_d) = \frac{e}{m_i} E, \tag{2}$$

$$\frac{\partial v_d}{\partial t} + v_d \frac{\partial v_d}{\partial x} + \nu_{dn} v_d + \nu_{di}(v_d - v_i) = \frac{Z_d e}{m_d} E, \tag{3}$$

*Permanent address: Institute of Radio Astronomy of the National Academy of Science of Ukraine, Chervonopraporna 4, Kharkov, Ukraine 61002.

 ©2004 The American Physical Society

$$\frac{\partial n_\alpha}{\partial t} + \frac{\partial}{\partial x}(v_\alpha n_\alpha) = 0. \tag{4}$$

Here v_α and n_α refer to the fluid velocities and densities of the different species ($\alpha = e, i, d$), having mass m_α, temperature T_α, and thermal velocities $v_{T\alpha} = \sqrt{T_\alpha / m_\alpha}$. Furthermore, E denotes the electric field, which includes the steady state (zero-order) dc field $E_0 = E_0 \hat{x}$. For simplicity of the subsequent analysis, the wave propagation is also considered along the x axis. Keeping in mind the application of our results for microgravity studies of complex plasma waves, Eq. (3) does not incorporate the gravitational force $F_g = m_d g$. Regarding the particle charges, we put $q_e = -q_i = -e$ for the plasma electrons and ions, while for the dust grains, the charge $q_d = eZ_d$ results from the electron and ion currents flowing to the dust grain surface.

Collisions with the neutral gas occur with collision frequencies $\nu_{en} \simeq n_n \sigma_{en} v_{Te}$, $\nu_{in} \simeq n_n \sigma_{in} v_{Ti}$, and $\nu_{dn} \simeq n_n \sigma_{dn} v_{Tn}$ for the electrons, ions, and dust particles, respectively (here n_n denotes the neutral number density and $\sigma_{\alpha n}$ is the effective collisional cross section). The others dissipative terms $\nu_{id}(v_i - v_d)$ and $\nu_{di}(v_d - v_i)$ account for the drag of the ions on the dust grains and *vice versa*, with ν_{id} being the ion-dust momentum-transfer frequency and $\nu_{di} = \nu_{id} m_i n_i / m_d n_d$ the dust-ion momentum-transfer frequency. Note that electron-ion and electron-dust collisions are not considered dynamically.

Finally, the set of equations (1)–(4) is closed by the Poisson equation for the electrostatic potential

$$\frac{\partial^2 \psi}{\partial x^2} = -4\pi e(n_i - n_e + Z_d n_d). \tag{5}$$

B. Equilibrium consideration

Letting $\partial/\partial t = \partial/\partial x = 0$ in the basic equations, Eq. (5) gives the charge neutrality condition

$$n_{0i} - n_{0e} + Z_d n_{0d} = 0, \tag{6}$$

while Eqs. (1)–(3) yield

$$v_{0e} = -\frac{e}{\nu_{en} m_e} E_0, \tag{7}$$

$$v_{0i} = \frac{e}{(\nu_{in} + \nu_{id}) m_i} E_0, \tag{8}$$

$$\nu_{dn} v_{0d} + \nu_{di}(v_{0d} - v_{0i}) = \frac{Z_d e}{m_d} E_0. \tag{9}$$

In typical experiments on low-frequency waves in complex plasmas under microgravity conditions, the dust particles do not reveal any visual drift inside a dust cloud. It is reasonable then to assume that, the ion drag is balanced by the electric force, yielding $v_{0d} = 0$ in Eq. (9). Elimination of the ion velocity v_{0i} between the two momentum equations (8) and (9) gives a simple relation between the dust charge density and collisional frequencies, viz,

$$\frac{\nu_{id}}{(\nu_{in} + \nu_{id})} = -\frac{Z_d n_{0d}}{n_{0i}}. \tag{10}$$

The equilibrium equations indicate that for stationary states of a homogeneous dusty plasma without dust flow, the ion-dust collision frequency ν_{id} (or ν_{di}) is not an independent plasma parameter but is self-consistently specified by the dust charge density. Introducing the Havnes parameter for ions $p_i = |Z_d| n_{0d} / n_{0i}$, it is possible to specify one of the most uncertain parameters in complex plasmas — the momentum-transfer frequency ν_{id} — as

$$\nu_{id} = \nu_{in} \frac{p_i}{1 - p_i}. \tag{11}$$

Moreover, the ion drift velocity is now determined by the momentum-transfer frequency ν_{in} and the ion Havnes parameter p_i,

$$v_{0i} = \frac{eE_0(1 - p_i)}{\nu_{in} m_i}. \tag{12}$$

C. Dispersion equation

Following the standard procedure, we linearize the basic equations (1)–(5) with respect to small perturbations $v_i \to v_{0i} + v_i$; $v_d \to v_d$, and $n_\alpha \to n_{0\alpha} + n_\alpha$; $\psi \to \psi_0 + \psi$, where the values with the subscript "0" refer to the equilibrium state of the plasma. All the first-order quantities are supposed to vary as $\propto \exp(-i\omega t + ikx)$. Introducing the susceptibilities for all plasma species as $\chi_\alpha = -4\pi q_\alpha n_\alpha / k^2 \psi$, and inserting these into the Poisson equation (5) gives the dispersion law

$$1 + \chi_i + \chi_e + \chi_d = 0. \tag{13}$$

Furthermore, we use the common assumption that compared to the heavy ions and dust grains, the plasma electrons can be considered as effectively massless. Then only the Boltzmann distribution

$$n_e = n_{oe} \exp\left(\frac{e\psi}{T_e}\right) \tag{14}$$

remains of Eq. (1) with an equilibrium electron density n_{oe}. This actually means that we have omitted the zero-order velocity for plasma electrons (7), which is justified when dealing with the plasma regime, corresponding to the ambipolar diffusion. The electron susceptibility reduces with the help of Eq. (14) to

$$\chi_e = \frac{1}{k^2 \lambda_{De}^2}, \tag{15}$$

where $\lambda_{De} = \sqrt{T_e / 4\pi e^2 n_{0e}}$ is the electron Debye radius.

The ion drift influence, on the other hand, will be kept in the main equations. Indeed, elimination of all quantities in favor of the ion density fluctuations n_i from Eqs. (2)–(5) yields

$$\chi_i = -\frac{\omega_{pi}^2}{(\omega - kv_{0i})(\omega - kv_{0i} + i\nu_i) - k^2 v_{Ti}^2} \tag{16}$$

with the effective ion collision frequency given by $\nu_i = \nu_{in} + \nu_{id}$ and the ion plasma frequency determined by $\omega_{pi}^2 = 4\pi e^2 n_{0i}/m_i$. For low frequencies $\omega \ll kv_{0i}$, we can neglect ω in comparison with kv_{0i} in Eq. (16). On the other hand, if the wave number satisfies the inequality

$$k < \frac{v_{0i}\nu_i}{v_{Ti}^2 - v_{0i}^2}, \tag{17}$$

the term $k^2(v_{Ti}^2 - v_{0i}^2)$ in the denominator of Eq. (16) can also be neglected and the ion susceptibility reduces to

$$\chi_i \simeq -i\frac{\omega_{pi}^2}{kv_{0i}\nu_i} = -i\frac{T_i}{k\lambda_{Di}^2 eE_0}, \tag{18}$$

where $\lambda_{Di} = \sqrt{T_i/4\pi e^2 n_{0i}}$ is the ion Debye radius.

Calculating in the same way the dust density perturbations n_d, one easily gets the dust susceptibility as

$$\chi_d = -\frac{\omega_{pd}^2}{\omega(\omega + i\nu_d)}. \tag{19}$$

Here the dust plasma frequency is $\omega_{pd} = \sqrt{4\pi Z_d^2 e^2 n_{0d}/m_d}$ and the effective collision frequency for the microparticles is introduced by $\nu_d = \nu_{dn} + \nu_{di}$. Usually, in complex plasmas $\nu_{dn} \gg \nu_{di}$ and, therefore, $\nu_d \sim \nu_{dn}$.

Substituting the derived plasma susceptibilities into Eq. (13) gives the dispersion relation

$$1 + \frac{1}{k^2\lambda_{De}^2} - i\frac{T_i}{k\lambda_{Di}^2 eE_0} - \frac{\omega_{pd}^2}{\omega(\omega + i\nu_{dn})} = 0. \tag{20}$$

A similar dispersion relation, but accounting for dust charge fluctuations in highly collisional complex plasmas, was recently discussed in connection with the ultra-low-frequency waves ($\omega < \nu_{dn}$) observed under microgravity conditions [15,20]. In the present analysis, we will concentrate on another limiting case, assuming that the wave frequency satisfies the inequality $\omega > \nu_{dn}$ or even $\omega \gg \nu_{dn}$. As will be shown later, this is the case in the latest experiments on plasma waves observed in the wave channel under microgravity.

Introducing a value $k_* = eE_0 n_{0e}/T_e n_{0i}$ with dimension of a wave number, we rewrite Eq. (20) as

$$1 + k^2\lambda_{De}^2 - i\frac{k}{k_*} - \frac{\omega_{pd}^2 k^2 \lambda_{De}^2}{\omega^2} \simeq 0. \tag{21}$$

D. Solutions of the dispersion relation

Inserting $\omega = \omega_r + i\omega_i$ into Eq. (21) gives two equations for the real and imaginary parts of the dispersion relation:

$$1 + k^2\lambda_{De}^2 - \frac{\omega_{pd}^2 k^2 \lambda_{De}^2 (\omega_r^2 - \omega_i^2)}{(\omega_r^2 + \omega_i^2)^2} \simeq 0, \tag{22}$$

$$\frac{k}{k_*} = 2\omega_r\omega_i \frac{\omega_{pd}^2 k^2 \lambda_{De}^2}{(\omega_r^2 + \omega_i^2)^2}. \tag{23}$$

This set of equations can be solved to yield the real and imaginary parts of the wave frequency,

$$\omega_{r,(i)}^2 = \frac{\omega_{pd}^2 k^2 \lambda_{De}^2}{2\sqrt{\frac{k^2}{k_*^2} + (1 + k^2\lambda_{De}^2)^2}} \left[1 \pm \frac{1 + k^2\lambda_{De}^2}{\sqrt{\frac{k^2}{k_*^2} + (1 + k^2\lambda_{De}^2)^2}} \right], \tag{24}$$

where the sign "plus" in the brackets corresponds to ω_r^2, while the "minus" sign is related to ω_i^2. The latter generalizes the solutions obtained in Ref. [20].

For wave numbers $k < k_*$ or $k > k^* = 1/k_*\lambda_{De}^2$, the general solution (24) represents a weakly growing ($\omega_r \gg \omega_i$) analog of the dust-acoustic mode, in which the role of the lighter component is played by the plasma electrons (the electron-dust-acoustic mode)

$$\omega_r^2 \simeq \frac{\omega_{pd}^2 k^2 \lambda_{De}^2}{1 + k^2\lambda_{De}^2}, \tag{25}$$

$$\omega_i^2 \simeq \frac{\omega_{pd}^2 k^4 \lambda_{De}^2}{4k_*^2(1 + k^2\lambda_{De}^2)^3}. \tag{26}$$

Since in complex plasmas typically $\lambda_{De}^2 \gg \lambda_{Di}^2$, the phase velocity of the perturbations (25) can be much higher than the usual dust-acoustic speed $u_{da} = \omega_{pd}\lambda_{Di}$.

In the case of intermediate wave numbers, $k_* < k < k^*$, the solution (24) is simplified to

$$\omega_{r,(i)} \simeq \frac{\lambda_{De}\omega_{pd}}{\sqrt{2}}\sqrt{k_* k}\left[1 \pm \frac{k_*(1 + k^2\lambda_{De}^2)}{2k} \right], \tag{27}$$

describing a highly unstable ($\omega_r \sim \omega_i$) dust density wave with nonacoustic dispersion $\omega \propto \sqrt{k}$ [20]. It is easily seen that for k, obeying $k < \lambda_{De}^2 k_*/2\lambda_{Di}^2 = eE_0/2T_i$, the phase velocity of the mode (27) exceeds u_{da}.

III. EXPERIMENT

The relevance of the calculated dust density perturbations [Eqs. (25)–(27)] for real dusty plasmas will now be investigated using the data obtained by the PKE-Nefedov laboratory onboard the International Space Station [21]. In these experiments, the plasma was produced in a symmetrically driven parallel plate capacitively coupled radiofrequency discharge. Plastic spherical grains of two different radii, $a = 1.7\ \mu$m and $a = 3.4\ \mu$m, were injected into an argon plasma. The microparticles formed two adjacent clouds between the electrodes with a lentil-shaped void (region free of particles) in the center of the chamber (Fig. 1). The inner small grain cloud (SGC) and the outer cloud formed by the larger particles (LGC) revealed ordered structures with average interparticle distances of 175 μm (SGC) to 270 μm (LGC). The argon background neutral pressure was 12 Pa, leading to dust-neutral collision frequencies $\nu_{dn} \sim 30\ \text{s}^{-1}$ and $15\ \text{s}^{-1}$ for small and large microparticles, respectively. Ap-

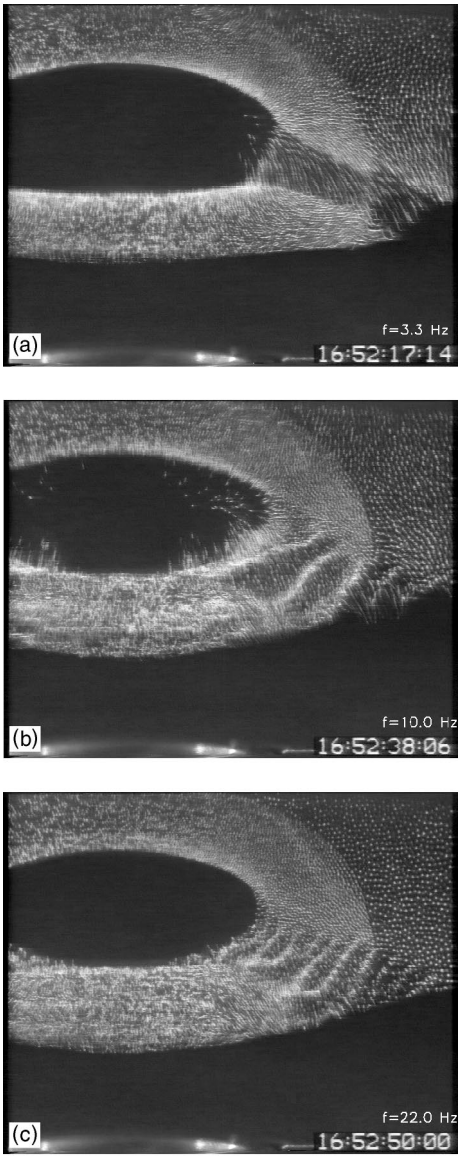

FIG. 1. Experimentally observed typical plasma structures and the wave channel at different excitation frequencies: 3.3 Hz (a), 10 Hz (b), and 22 Hz (c).

plying the previous calculations of the plasma densities in a argon discharge complex plasma under microgravity conditions [15] to the lower pressure the ion density is estimated to be in the range from $n_{0i} \sim 5 \times 10^8$ to 10^9 cm^{-3} in the vicinity of the SGC and $n_{0i} \sim 3 \times 10^8$ to 5×10^8 cm^{-3} in the cloud of larger particles. The electron temperature was about $T_e \sim 3$ eV, while for the ions $T_i \sim 0.03$ eV. The ion-neutral momentum transfer frequency can be estimated as $\nu_{in} \sim (2-2.5) \times 10^6$ s^{-1} and the ion-dust momentum transfer frequency ν_{id} we expect to be of the same order of magnitude as ν_{in} for both complex plasma domains. Such parameters indicate a complex plasma which could be considered to be highly collisional.

The important feature of the experiment is the presence of the void. Similar structures with the central void were observed in most of the experiments under microgravity conditions [15,21–25]. Presently it is believed that the main mechanism responsible for the void formation is the ion drag force, which can exceed the electrostatic force in the limit of weak electric fields and, hence, pushes the particles out of the central region of the discharge [26–29]. Inside the dust cloud the ion flow is decelerated by the ion-dust collisions (both absorption and scattering) and the ion drag force is reduced. This makes possible the existence of stationary dust cloud — inside the cloud the ion drag force is balanced by the electric force (as discussed in Sec. II B).

To make further progress in studies of the described complex plasma structures, a low-frequency modulational voltage was applied to the rf electrodes. The excitation frequency was varied by steps in the range from 2.7 Hz to 47 Hz. The grains were illuminated by a laser sheet perpendicular to the electrodes and imaged by a side video camera at 25 interlaced frames per second (fps). The video frames were recorded with a video camera and digitized, producing a sequence of images at 25 fps at a standard resolution (768×576 pixels).

This experiment would have been in many ways similar to the recently reported one [15] if the gas pressure was not two times lower. It turns out that a decrease in the neutral gas pressure can play a crucial role in complex plasma. It leads not only to the reduction in the dust-neutral collision frequency (by a factor of 2) and modifications in other plasma parameters as compared to Ref. [15], but the most surprising feature is an appearance of the specific waveguide in the complex plasma: when the positive part of the voltage fluctuation was superimposed to the electrodes, the void undergoes depletion, resulting in its opening through a narrow region—a wave channel. Figure 1 illustrates a typical picture of the specific plasma structures and the wave channel. The region inside the wave channel is highly interesting from the theoretical point of view because it exhibits density waves at different excitation frequencies in both plasma clouds formed by the smaller and larger particles [Figs. 1(b) and 1(c)]. Note that in the wave experiment of Ref. [15] only small grain cloud supported the density perturbations. The waves propagate in the direction of the electric field from the void boundary inside the complex plasma channel quite similar to wave disturbances in weakly ordered fluidlike complex plasmas. It is reasonable to assume that the double layer potential differences present at the boundaries between the void and different complex plasma regions $V \sim (1-2)T_e/e$ [23], are smoothed over the channel length, leading to an increase of the discharge electric field E_0 in this region. The values of E_0 can be roughly estimated as $(1-2)T_e/eL$, where L is a characteristic length of the plasma channel ($L \sim 0.8$ cm in SGC and $L \sim 0.4$ cm for LGC). This gives values of $E_0 \sim 5$ V/cm in the small grain cloud and $E_0 \sim 10$ V/cm in the large grain cloud.

Analyzing the recorded video sequences at the given frequency, we determined an average wavelength (wave number) and thus reconstructing the dispersion relation $\omega(k)$. Figure 2 shows the dispersion dependencies for the two different complex plasma clouds obtained by these means. It is seen that the wave perturbations are pronounced in different wave number domains: $30 \text{ cm}^{-1} < k < 100 \text{ cm}^{-1}$ (SGC) and $30 \text{ cm}^{-1} < k < 65 \text{ cm}^{-1}$ (LGC) and demonstrate nonacoustic

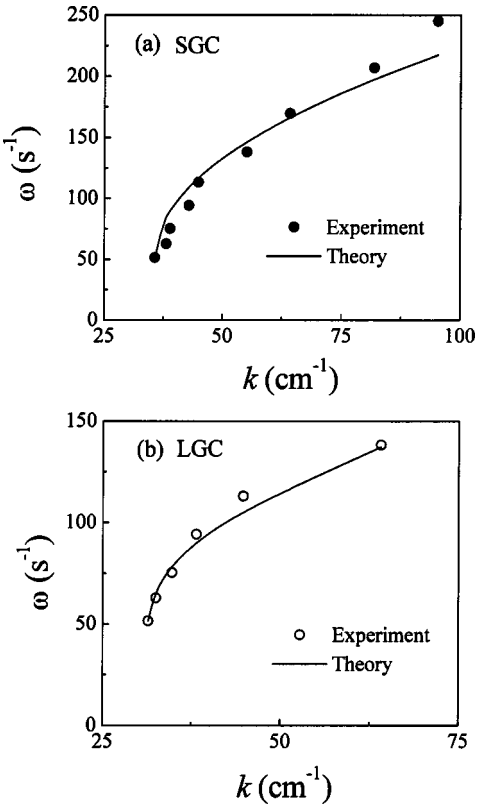

FIG. 2. Comparison of the experimentally measured dispersion relations with the theoretically predicted square root dependencies of Eq. (27). Plot (a) refers to the complex plasma formed by small grains (SGC), while plot (b) corresponds to the complex plasma domain formed by larger grains (LGC).

dependences $\omega(k)$ in both cases. One of the most interesting feature is the existence of a wave number range, where the density modes propagate at higher phase velocity in the larger grain plasma than in the medium of the smaller grains. Although the dispersion curves revealed different dispersion properties, the measured $\omega(k)$ dependences could be identified only for $\omega > \nu_{dn}$ in both cases. This is another principal difference when compared with the previous wave experiment [15], where the wave perturbations were observed only at $\omega < \nu_{dn}$. Finally note that the length scales of the observed waves, $\lambda = 2\pi/k \sim 0.2-0.06$ cm, are significantly shorter than the characteristic scales $L \sim (0.4-0.8)$ cm of the plasma channel. The latter can justify our one-dimensional approach for the description of the wave perturbations propagating along the wave channel.

Let us now consider the validity of the two different solutions [Eqs. (25)–(27)] from a standpoint of the aforementioned plasma parameters. We start with the analog of the electron-dust-acoustic mode (25). With an electric field $E_0 \sim 1-10$ V/cm and the assumption $n_{0i} \sim n_{0e}$ we get the maximal value of $k_* \sim 0.3-3$ cm^{-1}. The wavelengths associated with $k < k_*$ turn out to be very large ($\lambda \geqslant 2-20$ cm), far exceeding the dimensions of the complex plasma structures, while the observations revealed perturbations corresponding to $k \sim 30-100$ cm^{-1}. Another possibility for the solution (25) to exist requires $k > k^* = 1/k_* \lambda_{De}^2 = 4\pi e n_{0i}/E_0$. For the minimum applicable plasma density $n_{0i} \sim 5 \times 10^8$ cm^{-3} and rather large electric field $E_0 \sim 10$ V/cm, this gives $k^* \sim 100$ cm^{-1}. Larger plasma density and smaller electric field will lead to even larger k^*. Hence the electron-dust-acoustic mode (25) could manifest itself only in weakly ionized complex plasmas under moderate electric fields (e.g., $n_{0i} \leqslant 10^8$ cm^{-3} and $E_0 \sim 5$ V/cm leads to $k^* \leqslant 50$ cm^{-1}). It is unlikely that this mode is of importance for the discussed complex plasma experiment. So we have to use the square root solutions (27) appearing in the range $k^* > k > k_*$ which covers the range of observations in the experiment. Also, we take into account the possible difference in plasma parameters in SGC and LGC for interpretation of the experimental data in these two complex plasma domains separately.

A. Waves in a small grain cloud

Inside the small grain cloud the ion density is assumed to be close to its average value. Hence we use $n_{0i} \simeq 7 \times 10^8$ cm^{-3}, which leads to the ion Debye length $\lambda_{Di} \simeq 50$ μm. For definiteness, we put the electric field $E_0 \sim 5$ V/cm. The dust density can be estimated through the average particle separation $\Delta_s \sim 175$ μm in SGC, which gives $n_{d0} \simeq 1.9 \times 10^5$ cm^{-3}. As for the dust charge, the standard orbit motion limited approach (OML) predicts $Z_d^{\mathrm{OML}} \sim 5 \times 10^3$. However, we cannot rely on this estimation because of possible electron depletion in the dust cloud. Another important aspect is that we deal with a highly collisional case and ion charge exchange collisions can result in significant decrease of the grain charge in comparison with the OML predictions [30,31]. So the value of the dust charge has to be obtained by matching the measured dispersion curve (Fig. 2) with theoretically calculated dispersion relation (27) for the given plasma parameters.

Figure 2(a) shows the result of such matching. Very good qualitative agreement between measurements and theory is obtained in the range of wave numbers $k \sim 30-100$ cm^{-1} when the dust charge is of the order $Z_d \sim 3 \times 10^3$. The latter is almost half that estimated from the OML theory in qualitative agreement with Refs. [30,31].

The particle charge $Z_d \sim 3 \times 10^3$ immediately yields the dust plasma frequency $\omega_{pd} \simeq 450$ s^{-1}. Furthermore, substituting the ion and dust charge densities in Eq. (6) we find the electron density $n_{0e} \simeq 10^8$ cm^{-3} and the Debye length $\lambda_{De} \simeq 0.12$ cm. The ion Havnes parameter $p_i = |Z_d| n_{0d}/n_{0i}$ is then $p_i \simeq 0.85$ and the ion drift velocity (12) can be estimated as $v_{0i} \simeq 1.25 \times 10^4$ cm/s, which is a few times smaller than the ion thermal velocity $v_{Ti} \simeq 2.7 \times 10^4$ cm/s. These complex plasma parameters give the lower and upper limits of wave numbers as $k_* \simeq 0.3$ cm^{-1} and $k^* \simeq 200$ cm^{-1}, which cover the range of experimentally found wave numbers. Now we have only to check the validity of the specific form of the ion susceptibility (18). Putting appropriate values in Eq. (17) yields $k < 200$ cm^{-1}, which is the case.

B. Waves in a large grain cloud

It is reasonable to assume that the plasma density decreases outside the discharge central region and we can assume $n_{0i} \simeq 4 \times 10^8$ cm^{-3} inside the large grain plasma cloud,

while the electric field grows and we take $E_0 \sim 10$ V/cm. The ion Debye length is now $\lambda_{Di} \simeq 60$ μm and the dust density determined by the average particle separation $\Delta_L \sim 270$ μm is $n_{d0} \simeq 5 \times 10^4$ cm^{-3}. Since the size of the larger particle is twice the smaller one, we assume that the dust charge, carried by the particles in LGC is also twice the charge of the small grains, and hence $Z_d \sim 6 \times 10^3$. This leads to the dust plasma frequency $\omega_{pd} \simeq 170$ s^{-1}. The electron density can now be estimated as $n_{0e} \simeq 0.75 \times 10^8$ cm^{-3} and the Debye length $\lambda_{De} \simeq 0.14$ cm. The ion Havnes parameter becomes $p_i \simeq 0.82$ and the ion drift velocity (12) is of the same order as the thermal ion velocity $v_{0i} \simeq 2.7 \times 10^4$ cm/s. The lower and upper limits of the wave number are expected to be $k_* \simeq 0.7$ cm^{-1} and $k^* \simeq 70$ cm^{-1}, respectively. It should be pointed out that the inequality (17) is now fulfilled automatically, because $v_{Ti} \sim v_{0i}$.

Contrary to what has been done for the SGC, we will not match the dispersion curves, but just calculate Eq. (27) for the present plasma parameters and compare this with the experimental data. This could be considered as an additional verification of our interpretation. Comparison of the calculated dispersion relation (27) with the measured one is presented in Fig. 2. Very good qualitative agreement between the measurements and the calculations is seen over the whole range of wave numbers $k \sim 30-65$ cm^{-1}, supporting the presented theory.

IV. CONCLUSIONS

We have revised the linear dispersion relation, describing dust density perturbations in a highly collisional complex plasma with an ion drift, thus adapting this for realistic conditions in recent complex plasma experiments performed under microgravity conditions onboard the International Space Station. Dust density perturbations have been studied for wave frequencies larger than the dust-neutral momentum transfer frequency. Taking into account a relation between plasma parameters in an equilibrium state, two unstable modifications of the dust-acoustic mode have been obtained. The relevance of these perturbations to the observations of dust density waves in a specific wave channel has been analyzed. It is shown that a new mode, characterized by a square-root dependence of the wave frequency on the wave number, can satisfy the propagation conditions in the given range of wave numbers and thus can explain the peculiarities of the measured dispersion relation.

The comparison of the theory and the observations was made separately for two different complex plasma domains formed by small and large microparticles. Good qualitative agreement is found between the measured dispersion relations and the theoretically predicted square-root dependence of the wave frequency on the wave number in both domains. This allows a determination of the basic complex plasma parameters. We found that the grain charges in SGC and LGC are smaller than predicted by the OML theory. This is in qualitative agreement with recent studies of the effect of ion-neutral collisions on particle charging.

ACKNOWLEDGMENTS

V.V.Y. acknowledges the financial support of the Alexander von Humboldt Foundation (Germany) and Abdus Salam International Centre for Theoretical Physics (Italy). The work of B.M.A was supported by Das Bundesministerium für Bildung und Forschung durch das Zentrum für Luft- und Raumfahrt e.V. (DLR) unter dem Förderkennzeichen 50 RT 0207. This work was also supported by DLR/BMBF Grant No 50WM9852 and also partially by RFBR Grants Nos 01-02-16658, 03-02-16316, and 03-02-17240, as well as by INTAS Grants Nos 2000-0522 and 2001-0391. The authors acknowledge the excellent support of the PKE-Nefedov team.

[1] N. N. Rao, P. K. Shukla, and M. Y. Yu, Planet. Space Sci. **38**, 543 (1990).
[2] C. Thompson, A. Barkan, N. D'Angelo, and R. L. Merlino, Phys. Plasmas **4**, 2331 (1997).
[3] R. L. Merlino, A. Barkan, C. Thompson, and N. D'Angelo, Phys. Plasmas **5**, 1607 (1998).
[4] V. E. Fortov *et al.*, Phys. Plasmas **7**, 1374 (2000).
[5] V. Yaroshenko and G. Morfill, Phys. Plasmas **9**, 4495 (2002).
[6] V. V. Yaroshenko, F. Verheest, and M. Hellberg, Phys. Plasmas **10**, 3834 (2003).
[7] A. Samaryan, A. Chernyshev, O. Petrov, A. Nefedov, and V. E. Fortov, JETP **92**, 454 (2001).
[8] J. B. Pieper and J. Goree, Phys. Rev. Lett. **77**, 3137 (1996).
[9] G. E. Morfill, H. M. Thomas, and M. Zuzic, in *Advances in Dusty Plasmas*, edited by P. K. Shukla, D. A. Mendis, and T. Desai (World Scientific, Singapore, 1997), pp. 99–142.
[10] F. Melandsø, Phys. Plasmas **3**, 3890 (1996).
[11] A. Homann *et al.*, Phys. Rev. E **56**, 7138 (1997).
[12] A. Homann *et al.*, Phys. Lett. A **242**, 173 (1998).
[13] S. V. Vladimirov, P. V. Shevchenko, and N. F. Cramer, Phys. Rev. E **56**, R74 (1997).
[14] G. E. Morfill, A. V. Ivlev, and J. R. Jokipii, Phys. Rev. Lett. **83**, 971 (1999).
[15] S. Khrapak *et al.*, Phys. Plasmas **10**, 1 (2003).
[16] M. Rosenberg, in *Physics of Dusty Plasmas*, edited by P. K. Shukla, D. A. Mendis, and V. W. Chow (World Scientific, Singapore, 1996), p. 129.
[17] M. Rosenberg, J. Vac. Sci. Technol. A **14**, 631 (1996).
[18] N. D'Angelo and R. L. Merlino, Planet. Space Sci. **44**, 1593 (1996).
[19] M. Rosenberg, J. Plasma Phys. **41**, 229 (2001).
[20] S. A. Khrapak and V. V. Yaroshenko, Phys. Plasmas **10**, 4616 (2003).
[21] A. Nefedov *et al.*, New J. Phys. **5**, 33.1 (2003).
[22] G. E. Morfill *et al.*, Phys. Rev. Lett. **83**, 1598 (1999).
[23] B. M. Annaratone *et al.*, Phys. Rev. E **66**, 056411 (2002).
[24] A. V. Ivlev *et al.*, Phys. Rev. Lett. **90**, 055003 (2003).
[25] D. Samsonov *et al.*, Phys. Rev. E **67**, 036404 (2003).
[26] D. Samsonov and J. Goree, Phys. Rev. E **59**, 1047 (1999).
[27] J. Goree, G. E. Morfill, V. N. Tsytovich, and S. V. Vladimirov,

Phys. Rev. E **59**, 7055 (1999).
[28] S. A. Khrapak, A. V. Ivlev, G. E. Morfill, and H. M. Thomas, Phys. Rev. E **66**, 046414 (2002).
[29] E. Thomas, Jr., B. M. Annaratone, G. E. Morfill, and H. Rothermel, Phys. Rev. E **66**, 016405 (2003).
[30] A. V. Zobnin, A. P. Nefedov, V. A. Sinel'shchikov, and V. E. Fortov, JETP **91**, 483 (2000).
[31] M. Lampe, R. Goswami, Z. Sternovsky, S. Robertson, V. Gavrishchaka, G. Ganguli, and G. Joyce, Phys. Plasmas **10**, 1500 (2003).